Novelty Journals

ISSN 2394-9651

International Journal of Novel Research in Physics Chemistry & Mathematics
Vol. 11, Issue 2, pp: (72-84), Month: May - August 2024, Available at: www.noveltyjournals.com

Effects of Degradation on Photocatalytic Activity and Electronic Properties of $CuAl_2O_4$: A Density Functional Theory Study

Sattar H. Abed[1*], Ali H. Reshak[2]

[1]College of Education for Pure Sciences, University of Al-Muthanna, Al-Muthanna,Iraq.

[2]Physics Department, College of Science, University of Basrah, Basrah 61004, Iraq.

DOI: https://doi.org/10.5281/zenodo.13318659

Published Date: 14-August-2024

Abstract: **The study investigated the photocatalytic properties of the $CuAl_2O_4$ compound containing metal oxides. The X-ray diffraction analysis was used to refine the atomic arrangement in the material, and the Generalized Gradient Approximation (GGA-PBE) was applied in electronic and optical calculations using CASTEP code to analyze the structural composition of the compound. The optimized structure was utilized to compute the electronic structure and related properties. The study revealed that the calculated optical bandgap of the compound is 3.39 eV, enabling it to absorb light in the UV range. The electronic charge density distribution results showed a significant interaction between Al-O and Cu-O. The valence bands had substantial contributions from O_p and Al_d, while most of the energy levels in the conduction band were from Cu_d and Cu_s. This distribution enhances charge transfer and reduces recombination rates, thereby improving the efficiency of catalytic reactions. Based on these properties, the $CuAl_2O_4$ compound is considered a promising material for photocatalytic applications, opening new avenues for its use in photo reactive processes.**

Keywords: **$CuAl_2O_4$, GGA-PBE, Band Structure Electronic, photo degradation, DFT.**

1. INTRODUCTION

The environmental purification from pollution represents a critical and globally significant scientific issue essential for maintaining a healthy, pollutant-free environment [1-6]. The growing environmental concerns are largely attributed to industrial hazards, with manufacturing waste and harmful energy sources contributing approximately 20% of water contamination [4-9]. Liquid waste, laden with diverse organic, chemical, and biological contaminants, poses a substantial threat to both human health and the environment [9,10–16]. While various methods have been developed to convert hazardous waste into manageable forms, most are costly and energy-intensive. In this context, semiconductor photocatalysis has emerged as a promising, eco-friendly technique for effectively removing harmful pollutants from wastewater [17-21]. The chemical stability of materials plays a crucial role in their suitability for photocatalytic applications aimed at decomposing organic waste [24-27]. Recent studies have highlighted the significant impact of nanoparticle composition on their ability to catalyze chemical reactions through light [28–35]. Over recent years, metal oxide compounds have garnered substantial interest due to their advantageous optical and electronic properties, making them ideal candidates for a variety of applications. Among these, $CuAl_2O_4$ stands out as a chemically stable material with minimal internal defects, excellent optical response, and effective light absorption. Furthermore, its appropriate energy bandgap, abundance, and cost-effectiveness render it particularly suitable for photovoltaic and photocatalytic applications [12, 24].

The compound $CuAl_2O_4$ consists of two copper atoms, four aluminum atoms, and eight oxygen atoms, crystallizing in a moderately cubic crystal system, specifically within the Fd-3m space group. This space group defines the symmetry and arrangement within the crystal, imparting distinctive geometric and organizational properties to the material [34].The

density Functional Theory (DFT) is a precise computational method utilized to explore the photocatalytic mechanisms of $CuAl_2O_4$. In this study, the Generalized Gradient Approximation (GGA-PBE) was applied for electronic and optical calculations using the CASTEP code [40-43]. The results revealed that the optimized structure of $CuAl_2O_4$ exhibits a direct bandgap of 3.39 eV, which closely matches values obtained from various approximate methods [46-50,23].The analysis of the supercell structure of $CuAl_2O_4$ demonstrated that the compound, with its specific Cu-O and Cu-Al bond distances and an energy bandgap of 3.39 eV, effectively absorbs light in the ultraviolet range.

Additionally, the electronic charge density distribution showed significant interactions between Al-O and Cu-O, with notable contributions from O_p and Al_d in the valence band, while Cu_d and Cu_s dominate the conduction band. Moreover, the study indicates that the photocatalytic activity of $CuAl_2O_4$ has considerable potential in redox reactions, with valence band and conduction band potentials determined at 0.28126 eV and 3.68024 eV, respectively. These findings underscore the compound's effectiveness in meeting the demands of photocatalytic applications, making it an excellent material for water purification and hydrogen production.

2. COMPUTATIONAL METHODOLOGY

The study employed the CASTEP algorithm to analyze the electrical and structural properties of $CuAl_2O_4$, a material comprising 86 atoms, using Density Functional Theory (DFT) to assess its photocatalytic efficiency, yielding highly accurate results. This systematic approach in computational problem-solving and analysis is essential [41]. The calculations were based on crystallographic data from single-crystal X-ray diffraction, utilizing the generalized gradient approximation with the Perdew-Burke-Ernzerhof parameterization [42,43]. The interactions between ionic cores and valence electrons were described using a norm-conserving pseudopotential [40]. The Brillouin zone was sampled using a Monkhorst-Pack k-point mesh and a plane wave basis with an energy cut-off of 440 eV. Convergence criteria for atomic forces and mass were set with thresholds of 0.0483 eV.

3. RESULTS AND DISCUSSION

3.1 Structural properties

The copper aluminate ($CuAl_2O_4$) belongs to the space group F d -3 m (No. 227), representing the cubic phase of the crystal lattice, as shown in Table (1) (JCPDS card No. 01-077-2494). The lattice constants were experimentally determined and subsequently optimized using the generalized gradient approximation (GGA-PBE), as illustrated in Fig.1 [50, 51]. It can be observed that there is a close agreement between the experimental and theoretically optimized results, indicating high accuracy in the arrangement of atoms, internal angles, and crystal packing [52]. The figure from arrangement indicates an ordered crystal structure, enhancing the properties of the compound as an effective photocatalytic material. The figure represents an optimization process analyzing the convergence of energy, displacement, and maximum force criteria. The blue line shows a sharp decrease in energy change, indicating system stabilization. The orange and purple lines display gradual decreases in maximum displacement and force, respectively, reflecting the stabilization of atoms and forces. Demonstrates the effectiveness of the optimization in converging the system toward a more stable state, though additional steps are required for full convergence. the precise geometric arrangement of the atoms plays a crucial role in the compound's interaction with light and photocatalytic reactions.

Table (1) It data on the structural properties of the compound $CuAl_2O_4$.

JCPDS card No. 01-077-2494					
Lattice type F Space group name F d -3 m Space group number 227					
Lattice parameters					
a(Å)	b(Å)	c (Å)	α	β	γ
8.07500	8.07500	8.07500	90°	90°	90°
Unit-cell volume = 529.535385 $Å^3$					

Novelty Journals

ISSN 2394-9651

International Journal of Novel Research in Physics Chemistry & Mathematics
Vol. 11, Issue 2, pp: (72-84), Month: May - August 2024, Available at: www.noveltyjournals.com

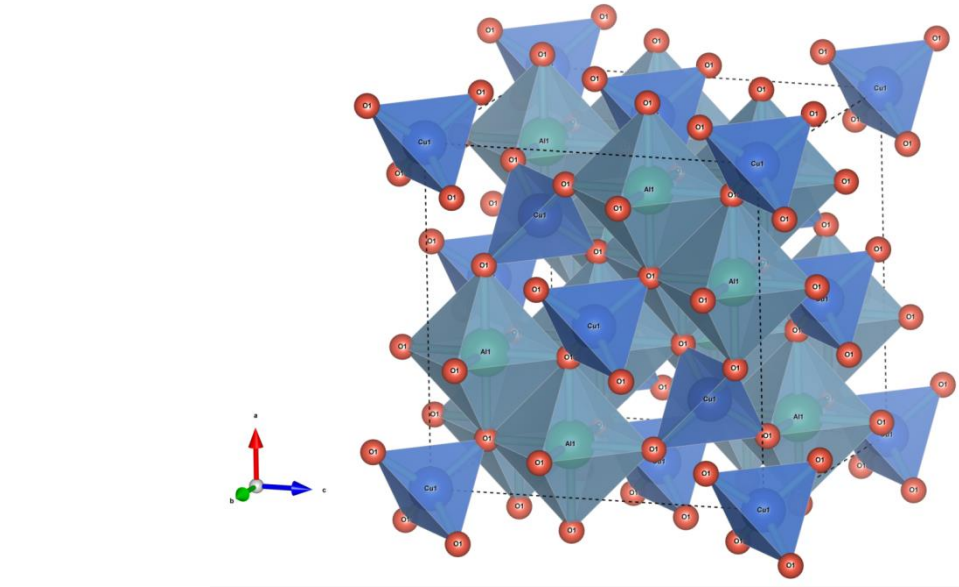

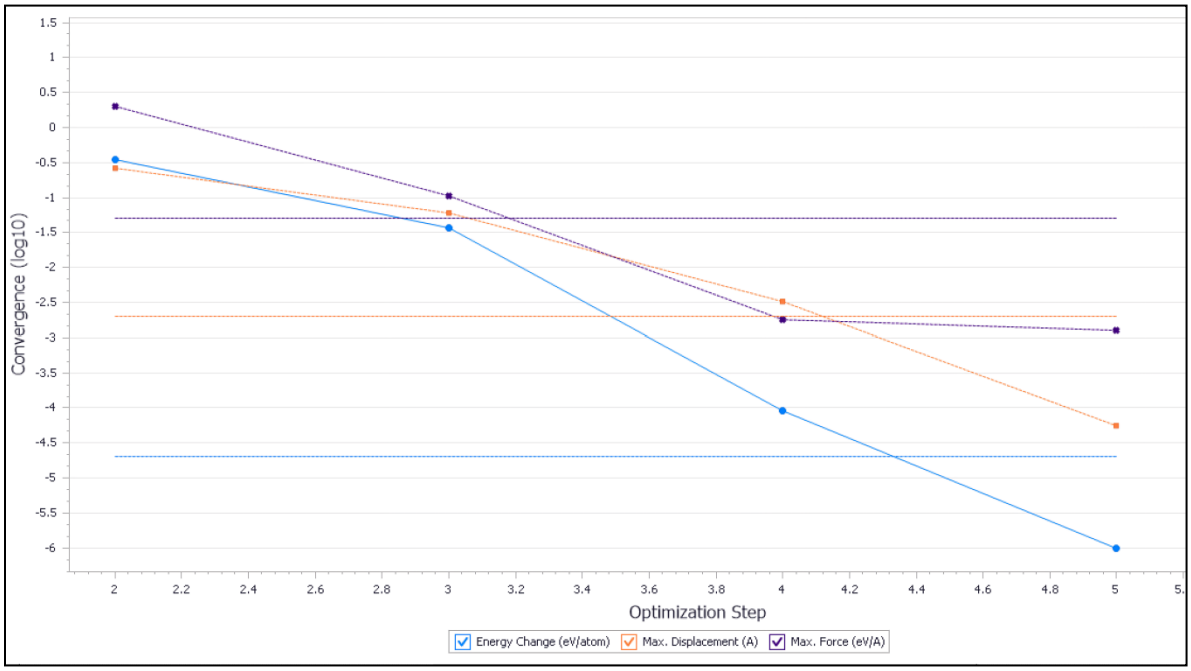

Fig.(1): (a) The crystal structure and arrangement of atoms of the compound $CuAl_2O_4$. (b) Analysis of convergence in energy, displacement, and maximum force during optimization.

3.2. Electronic properties

3.2.1 Band Structure Electronic

The electronic to study behavior of $CuAl_2O_4$, the electronic band structures and The total and partial densities of states were computed using several potentials, including GGA-PBE. The plots are displayed in fig. (2,3), correspondingly. The fermi energy level (E_F) is defined as 0eV for all computations. This energy level corresponds to both the highest energy level in the valence band (VB) and the lowest energy level in the conduction band (CB).

The band structure is a crucial characteristic in the field of solid-state physics, since it directly or indirectly influences all physical properties of materials through the band gap. The results obtained for $CuAl_2O_4$ show that the valence band maximum (VB_M) and conduction band minimum (CB_M) lie on one (K-point) G, A,H, K,M and L. The semiconducting

Novelty Journals

ISSN 2394-9651

International Journal of Novel Research in Physics Chemistry & Mathematics
Vol. 11, Issue 2, pp: (72-84), Month: May - August 2024, Available at: www.noveltyjournals.com

compound has an energy gap direct and indirect, and this result is identical to the experimental results, the compound has a false direct energy gap of 3.46 eV[53,5]. The energy of the compound, other experimental and theoretical works are shown in table (2). The metallic behavior of this material, metal oxide.

Table (2) The energy gap is the experimental and theoretical $CuAl_2O_4$ results.

Compound	Present work	Res.
	Theoretical	Experimental
$CuAl_2O_4$	3.39eV	3.46 eV

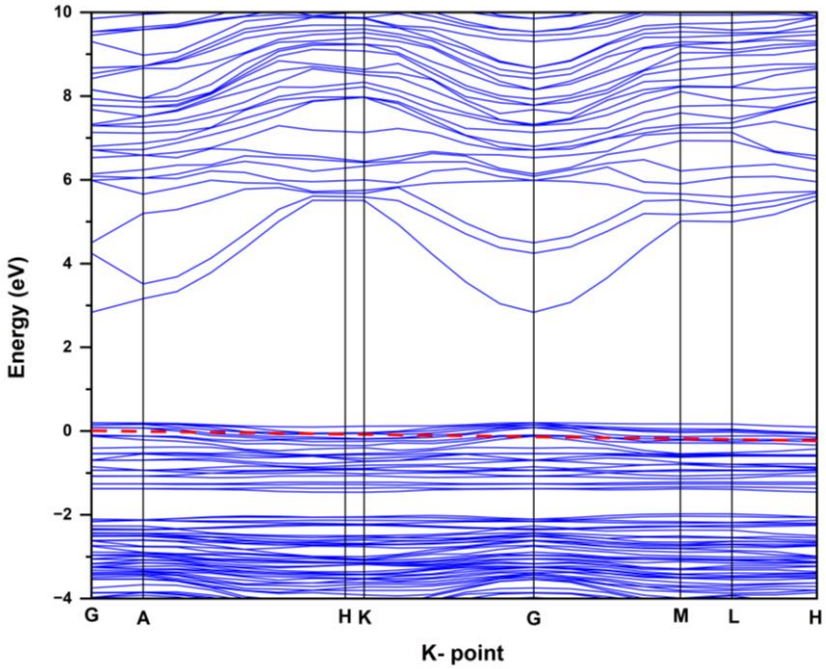

Fig. (2) The electronic band structure of a compound $CuAl_2O_4$.

3.2.2. Total Density of States (TDOS) and Partial Density of States (PDOS).

The band structure of $CuAl_2O_4$ compounds, analyzed using different cross-linking potentials, shows minimal variation from actual results, with the spin-orbital interaction being the primary factor influencing these materials. Theoretical analysis of electronic band structures and their impact on electron energy levels is elucidated through the density of states (DOS).

Fig.3(a) illustrates the total density of states (TDOS) for $CuAl_2O_4$, with the energy range from (-8_12) eV. The valence band is indicated by negative values, and the conduction band by positive values. The energy gap is approximately 3.38 eV, with zero density at the fermi level (E_f = 0 eV). Multiple peaks at negative energies indicate concentrated electronic states, while the conduction band shows a gradual increase in density with several peaks, the highest between 10.40 eV and 12 eV. The partial density of states (PDOS) for $CuAl_2O_4$ reveals specific contributions from each element (Cu-3d) orbitals significantly contribute to the valence band (-7 _ 0)eV, while (Al-3d) orbitals, although less prominent, contribute to the compound's electronic properties. The oxygen's orbitals (O-2p) significantly contribute to the valence band, enhancing chemical bonding and charge transfer. The valence band (VB) contains a high density of states, primarily from (Cu-3d) and (O-2p) orbitals, within the energy range of (-6 _ 0) eV. The conduction band (CB) starts from 0 eV, with contributions from Cu and Al orbitals increasing with energy. The energy gap between the filled and empty states is critical, with orbitals near the fermi level, particularly (Cu-d) and (Al-p) orbitals, playing a decisive role in the photocatalytic process. $CuAl_2O_4$ exhibits semiconducting properties, making it suitable for photocatalytic applications, where orbitals (Cu-d) are crucial for photoabsorption and catalytic activity, and orbitals (O-2p) significantly impact chemical reactions and bond formation.

Novelty Journals

ISSN 2394-9651

International Journal of Novel Research in Physics Chemistry & Mathematics
Vol. 11, Issue 2, pp: (72-84), Month: May - August 2024, Available at: www.noveltyjournals.com

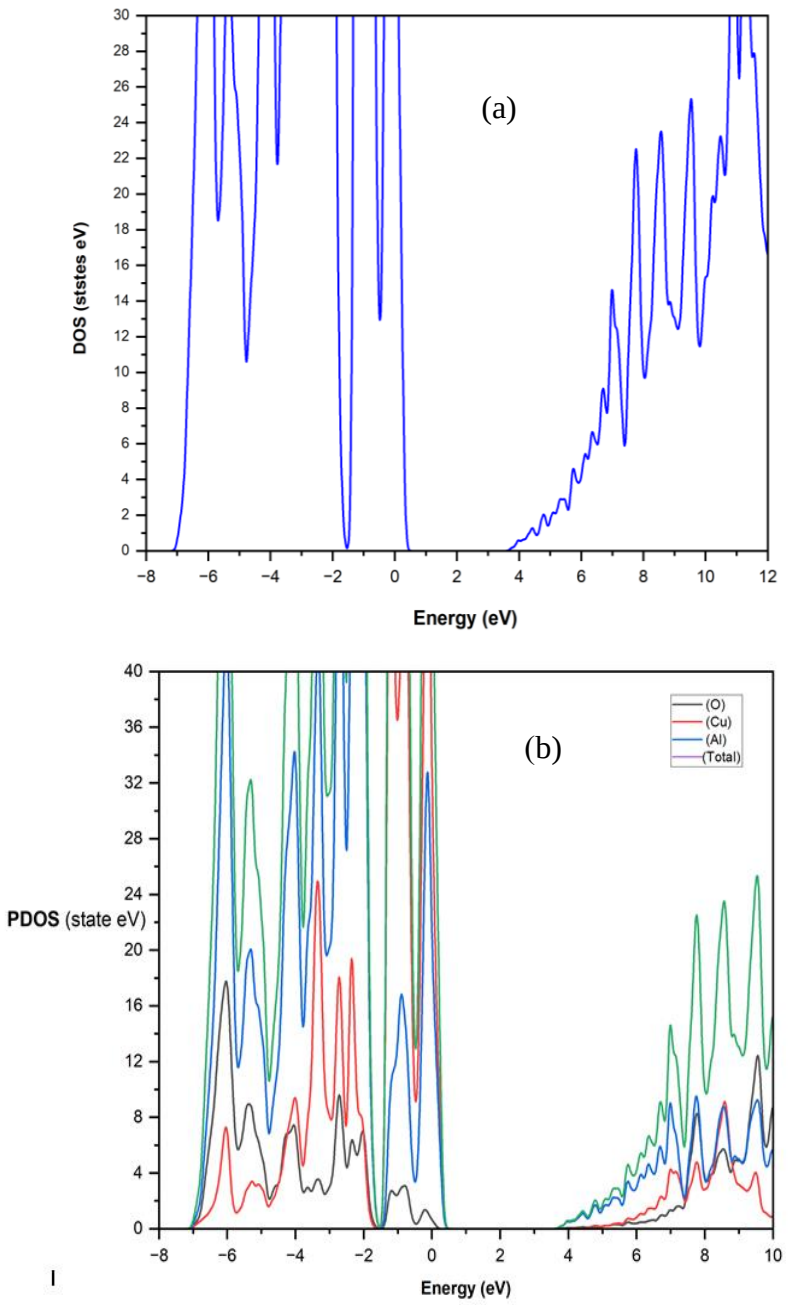

Fig.(3): (a) The total density of states (TDOS), (b) The Partial density of states (PDOS).

3.3. Optical properties results

The study of the optical properties of $CuAl_2O_4$ reveals several key findings crucial for its potential applications. $CuAl_2O_4$ exhibits a direct bandgap of 3.39 eV, indicating its activity in the UV region, which is advantageous for optical detectors and photo-stimulated devices. The dielectric function of $CuAl_2O_4$ shows a high peak in the real part at low energies (0-5)eV, suggesting strong dielectric behavior and respons-iveness to external electric fields, which stabilizes at lower values at higher energies (5-30)eV with minor oscillations. The imaginary part of the dielectric function reveals prominent peaks around 3 eV, signifying significant energy absorption due to electronic transitions, with a gradual decrease at higher energies (5-30)eV.

In terms of refractive index and extinction coefficient, the refractive index starts high (6.5) at near-zero energies, decreases sharply, and stabilizes between (1.5_2.5)eV, eventually reaching lower values at higher energies (15-30)eV.

The extinction coefficient begins at low values, peaks around 2 eV, and then decreases gradually, with a second peak around 15 eV before nearing zero. The energy loss function, spanning from 0 to 20 eV, starts with very low values, remains close to zero until about 20 eV, sharply increases around 23 eV, peaks near 25 eV, and then rapidly decreases to near zero around 27 eV, indicating strong electron-photon interactions and effective energy absorption in this range.

The conductivity variations show that the real part of conductivity increases gradually at low energies, peaks at 13.56 eV, rises significantly at intermediate energies, peaks at 14.73 eV, and then declines sharply. The imaginary part of conductivity starts near zero, decreases to -0.573 at 1.275 eV, then rises again, peaking at 20 eV before gradually decreasing after 25 eV, as in the fig. 4(a,b,c,d,e). These optical properties position $CuAl_2O_4$ as a promising candidate for photocatalytic applications, including water splitting, organic pollutant removal, and enhancing solar cell efficiency. The stable dielectric response and refractive index at various energy ranges support its effectiveness in photonic excitation and catalytic processes. Additionally, the peaks in the extinction coefficient and energy loss function suggest efficient energy absorption and electron excitation, which are crucial for photochemical reactions.

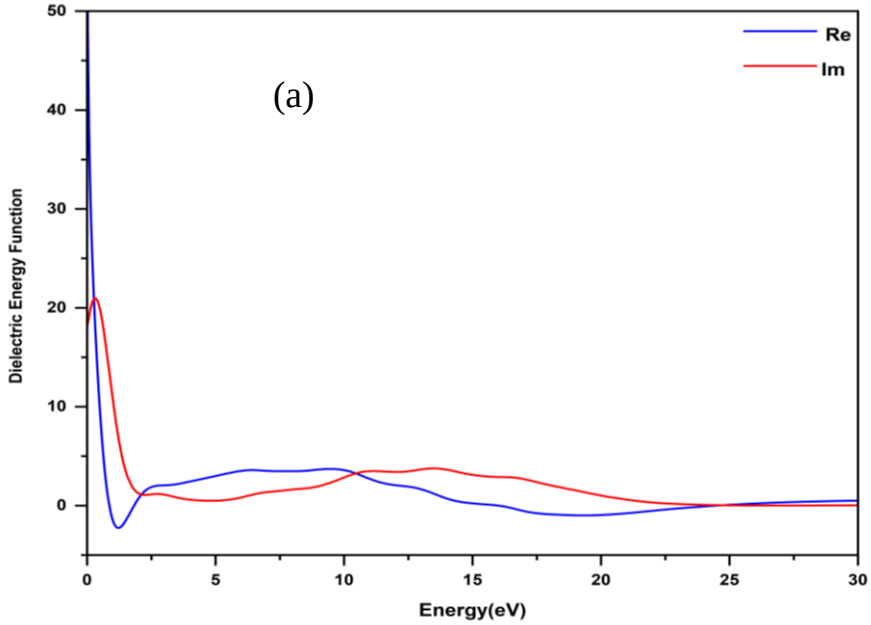

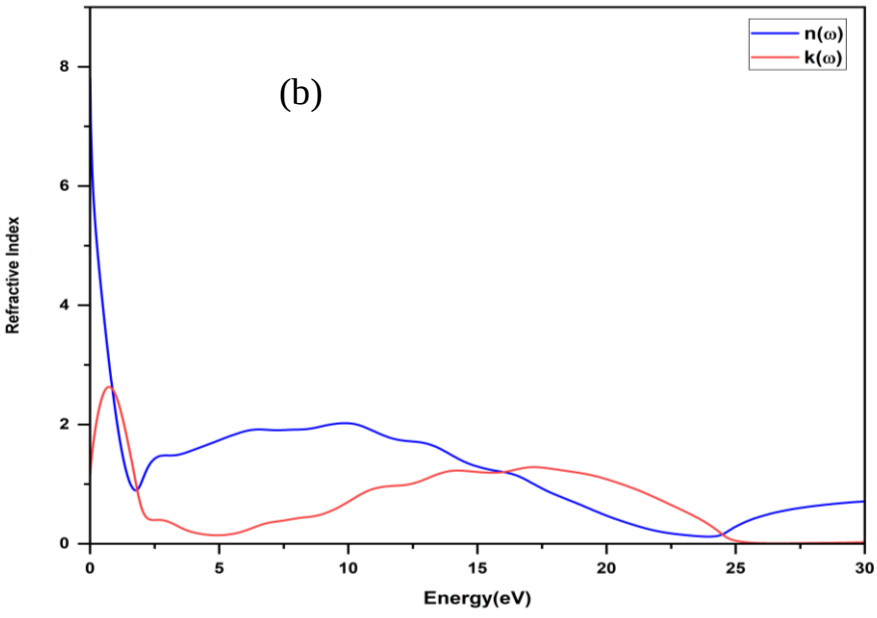

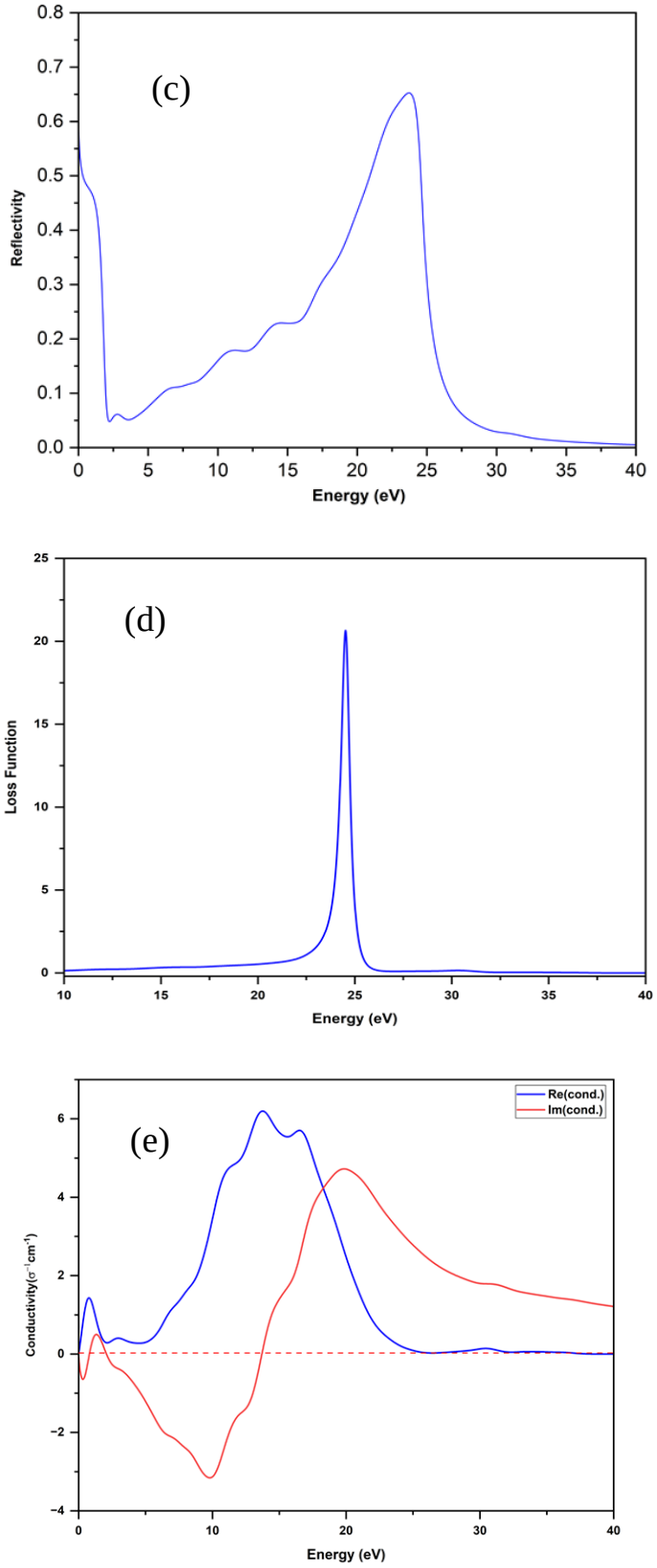

Fig.4 The calculated Optical properties of $CuAl_2O_4$ by method (GGA-PBE): (a) The Real $\varepsilon_1(\omega)$ and Imaginary $\varepsilon_2(\omega)$ dielectric functions, (b) the refractive index n(ω) and extinction coefficient k(ω), (c) The calculated reflectivity, (d) The energy loss function (ELF), (e) The conductivity.

Novelty Journals

ISSN 2394-9651

International Journal of Novel Research in Physics Chemistry & Mathematics
Vol. 11, Issue 2, pp: (72-84), Month: May - August 2024, Available at: www.noveltyjournals.com

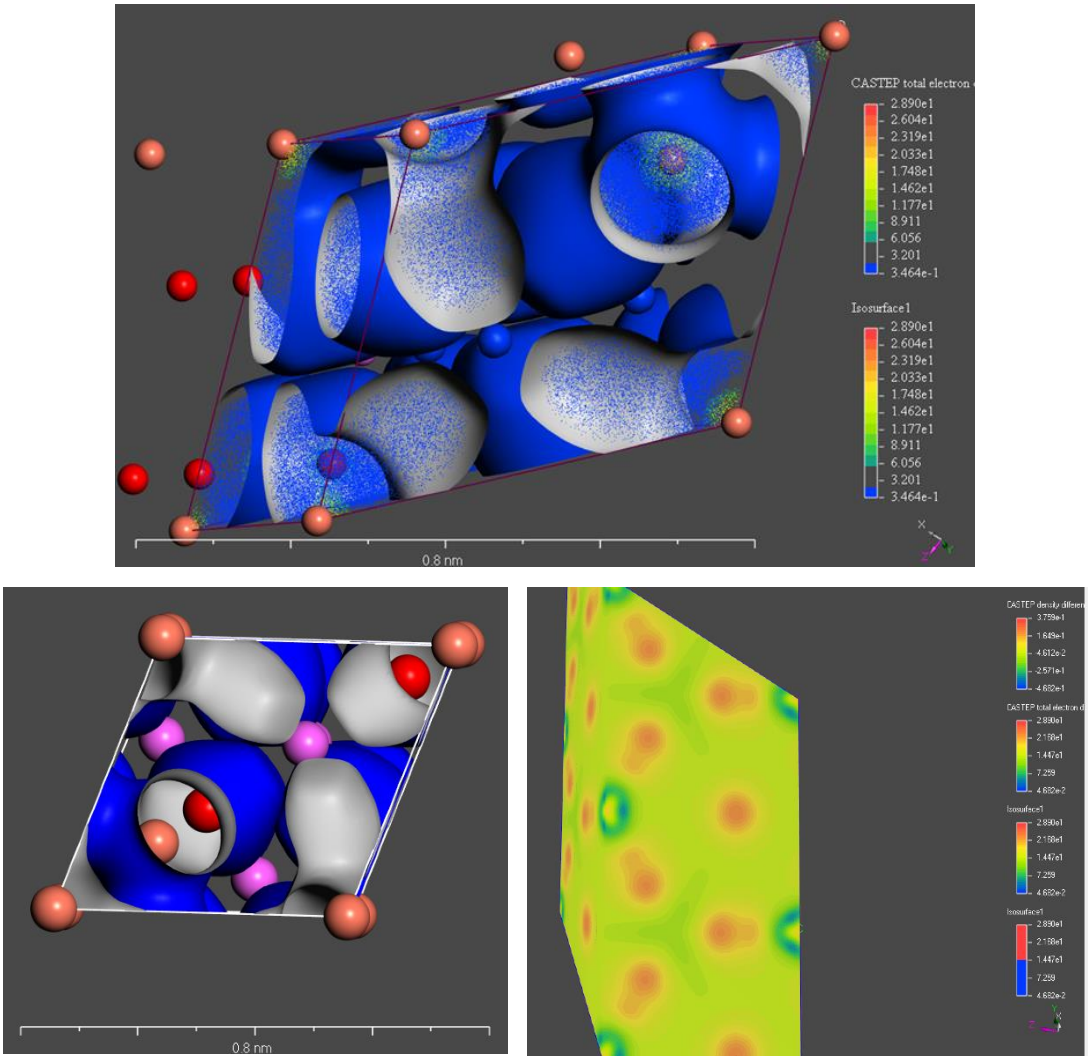

Fig. (5) The charge density to compound $CuAl_2O_4$ by method (GGA-PBE).

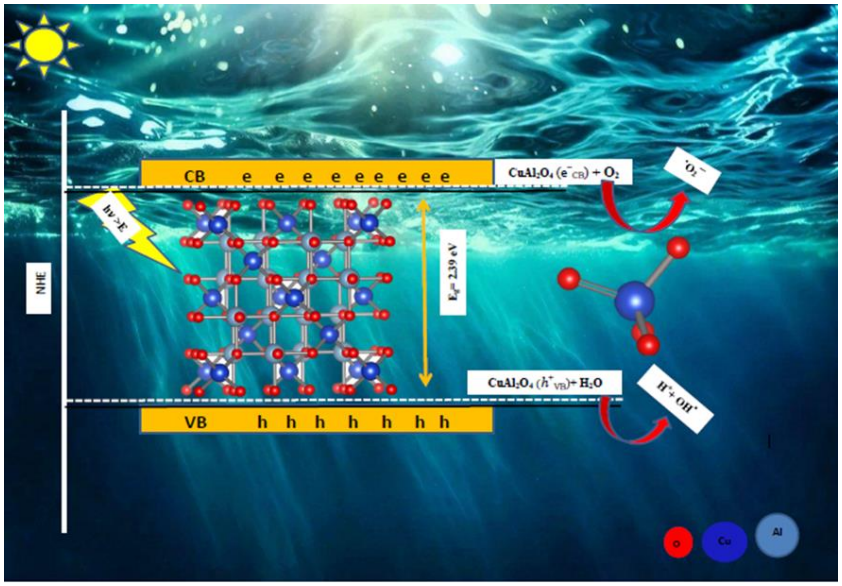

Fig.(6): Photocatalytic mechanism of $CuAl_2O_4$ compounds for organic dye degradation by using ultraviolet radiation.

Novelty Journals

ISSN 2394-9651

International Journal of Novel Research in Physics Chemistry & Mathematics
Vol. 11, Issue 2, pp: (72-84), Month: May - August 2024, Available at: www.noveltyjournals.com

3.4. photodegradation

In order to get a deeper understanding of the experimentally reported results, a computational analysis based on density functional theory (DFT) was conducted. This work involved creating an orthorhombic supercell of $CuAl_2O_4$. The supercell structure of $CuAl_2O_4$, which has been improved, the mean bond distance between Cu-O in this study is 1.74829Å and Cu-Al is 2.01875Å, which closely corresponds to previously documented measurements. The efficacy of dye degradation in a nanoparticle can be assessed by utilizing a limited number of factors derived from DFT simulations[45,55].

The developed supercell has a visible area bandgap value of 3.39eV in the present study. The PDOS spectrum in fig.(3) demonstrates the orbital impact of the Cu, Al and O atoms. The figure clearly demonstrates that the presence of (O_p) and (Al_d) orbitals has a significant impact on the valence band. However, the (Cu_d),(Cu_s) orbitals on the conduction band side provide the majority of the energy levels. These orbitals facilitate the transmission of electric charge between the valence and conduction bands. In addition, there are a lot of different energy states in both the valence and conduction bands.

The redox capability of $CuAl_2O_4$ can be attributed to the band edge potentials, which have a pivotal role in oxidation and reduction reactions. The band edge potentials for the $CuAl_2O_4$ nanostructure are determined using the following equations[51, 55-57].

$$E_{vb} = \chi - E_e + \frac{1}{2}(E_g)$$
$$E_{cb} = E_{vb} - E_g$$

Here, Eg designates the calculated energy difference, and χ represents the electronegativity. The valence band and conduction band edge potentials have been determined to be 0.28126eV and 3.68024 eV, respectively. The $CuAl_2O_4$ calculated band edge potentials meet the requirements for a good photocatalytic material[55]. The valence band potential (PH = 0) is 0.28126eV, and the conduction band edge is 3.68024eV. The relevant potentials mentioned are the standard normal hydrogen electrode (NHE) potentials used for scaling efficient photocatalytic materials, According to the equation, the voltage edge for the equalization and conduction bands (NHE) and at PH = 7 is as follows [56,58]:

$$E_{cb}(\mathrm{NHE}) = E_{Cb}(\mathrm{PH} = 0) - 0.059 * \mathrm{PH}$$
$$E_{vb}(\mathrm{NHE}) = E_{vb}(\mathrm{PH} = 0) - 0.059 * \mathrm{PH}$$

The Charge free carrier mobility is employed as a measure to assess the photocatalytic activity of $CuAl_2O_4$. The increase mobility of the charge carriers results in a reduction in the rate of recombination, hence enhancing the rates of redox reactions, to quantify mobility, one can determine the effective mass (m^*) of the charge carriers. Based on the findings in the literature [56-58]. It is necessary for the effective mass of charge carriers in a nanomaterial to be less than 0.5me in all crystallographic orientations.

This leads to a reduction in the diffusion coefficient, resulting in a drop in the rate of recombination. An in-depth understanding of the Distribution of the electronic charge density of the compound $CuAl_2O_4$ by the density functional theory (DFT) (GGA-PBE) to calculate the charge density of the expected compound atoms on the (311) plane, as in fig. (5).

A figure representing the distribution of electronic charge density, where different colors indicate various charge densities. Red represents high charge density, while blue represents low charge density. In this figure, the red regions reflect large clusters of electrons centered around basic atoms such as copper and aluminum, while the blue regions show low charge density in the spaces between the atoms.

Crystal structure plays a crucial role in this distribution, as heavy atoms show high charge density while voids show low density. This distribution has a significant impact on physical processes such as redox during photocatalysis. Regions with high density contribute to reduction processes easily due to the abundant availability of electrons, while regions with low density are good centers for oxidation processes due to the lack of electrons and the presence of holes. This distribution enhances the photocatalytic efficiency of the $CuAl_2O_4$ compound, making it a useful material in water purification and

hydrogen production. Understanding the charge density distribution helps improve the performance of materials in photocatalysis by identifying the most effective regions for chemical reactions, as in the fig. (6).

The optimal distribution of electronic charges enhances the efficiency of the $CuAl_2O_4$ compound in photocatalysis. The detailed distribution of electronic charges provides deep insight into how to improve the efficiency of photocatalytic materials and increase their effectiveness in diverse applications. $CuAl_2O_4$ appears as a distinguished choice thanks to its ideal distribution of charges that enhances the effectiveness of photochemical reactions, which enhances its ability to perform photocatalysis efficiently in redox processes, which increases the efficiency and effectiveness of its use in various photocatalytic applications.

4. CONCLUSIONS

The study investigated the use of $CuAl_2O_4$ as an active photocatalyst using the DFT (PBE-GGA) method. It was concluded that computational analyses using the GGA-PBE approximation for the crystal structure of $CuAl_2O_4$ show notable optical and electronic properties. The calculated optical bandgap of 3.39 eV (365.78 nm) for the incident light highlights its suitability for photocatalytic applications. The partial density of states (PDOS) spectra indicate significant contributions from O_p and Al_d orbitals in the valence band, while Cu_d and Cu_s orbitals dominate the conduction band. The band edges, determined at 0.28126 eV for the valence band and 3.68024 eV for the conduction band, suggest that $CuAl_2O_4$ meets the criteria for effective photocatalysis. The charge density distribution shows high electron density around the Cu-O and Al-O atoms, enhancing chemical reactions and photocatalytic efficiency. This distribution improves the effectiveness of $CuAl_2O_4$ in catalytic processes such as the purification of polluted and biological water and the production of renewable energy (hydrogen).

ACKNOWLEDGEMENTS

The authors gratefully acknowledge support from department of Physics, College of Science, University of Basrah, Iraq.

Author Contributions: Sattar H. Abed wrote the main manuscript text and prepared all figures. Ali H. Reshak supervised the manuscript and edited the manuscript.

Ethical Approval: The study protocol was approved by local ethics committee.

Disclaimer: None

Conflict of interest: There are no conflicts of interest to declare.

Funding disclosure: support by ourselves.

REFERENCES

[1] J. Kaur, T. Pathak, A. Singh, and K. Kumar, "Application of nanotechnology in the environment biotechnology," in Advances in Environmental Biotechnology , Springer, 2017, pp. 155-165.

[2] J. Zhang, B. Tian, L. Wang, M. Xing, and J. Lei, Photocatalysis: Fundamentals, Materials and Applications, vol. 100. Springer, 2018.

[3] M. Pelaez et al., "A review on the visible light active titanium dioxide photocatalysts for environmental applications," Appl. Catal. B Environ. , vol. 125, pp. 331-349, 2012, doi: 10.1016/j.apcatb.2012.05.036.

[4] H. S. Lee, J. Lee, S. Lee et al., "Walnut-like ZnO-Zn_2TiO_4 multicore shell submicron spheres with a thin carbon layer: fine synthesis; facile structural control and solar light photocatalytic application," Acta Material, vol. 122, pp. 287-297, 2017.

[5] S. H. Abed and A. H. Reshak, " "Enhancing the Photocatalytic Efficiency of $CuAl_2O_4$ Nanoparticles: Effective Degradation of Organic Dyes under Ultraviolet Light"," J. F

[6] N. N, Z. L, F. J et al., "Self-assembled hierarchical direct Z-scheme g-C_3N_4: ZnO microspheres enhanced photocatalytic CO_2 reduction performance," Applied Surface Science, vol. 441, pp. 12-22, 2018.

[7] O. Legrini, E. Oliveros, and A. M. Braun, "Photochemical processes for water treatment," Chem. Rev. , vol. 93, no. 2, pp. 671-698, 1993.

[8] N. Luis and J.-A. Wang, Advanced Catalytic Materials: Photocatalysis and Other Current Trends. BoD-Books on Demand, 2016.

[9] C. Byrne, G. Subramanian, and S. C. Pillai, "Recent advances in photocatalysis for environmental applications," J. Environ. Chem. Eng. , vol. 6, no. 3, pp. 3531-3555, 2018.

[10] K. Sharma, A. S. Al-Kabbi, G. S. S. Saini, and S. K. Tripathi, "Indium doping induced modification of the structural, optical and electrical properties of nanocrystalline CdSe thin films," J. Alloys Compd. , vol. 564, pp. 42-48, 2013, doi: 10.1016/j.jallcom.2013.02.037.

[11] K. A. Mohammed et al., "Optical, morphological, electrical properties and white light photoresponse of CdSe nanoparticles," Adv. Mater. Process. Technol. , vol. 8, no. sup4, pp. 2289-2298, 2022, doi: 10.1080/2374068X.2022.2037877.

[12] T. Oyama, A. Aoshima, S. Horikoshi, H. Hidaka, J. Zhao, and N. Serpone, "Solar photocatalysis, photodegradation of a commercial detergent in aqueous TiO_2 dispersions under sunlight irradiation," Sol. Energy , vol. 77, no. 5, pp. 525-532, 2004.

[13] M. R. Khan, T. W. Chuan, A. Yousuf, M. N. K. Chowdhury, and C. K. Cheng, "Schottky barrier and surface plasmonic resonance phenomena towards the photocatalytic reaction: study of their mechanisms to enhance photocatalytic activity," Catal. Sci. Technol , vol. 5, no. 5, pp. 2522-2531, 2015.

[14] H. Kisch, "Semiconductor photocatalysis - mechanistic and synthetic aspects," Angew. Chem. Int. Ed. , vol. 52, no. 3, pp. 812-847, 2013.

[15] J. Li and N. Wu, "Semiconductor-based photocatalysts and photoelectrochemical cells for solar fuel generation: a review," Catal. Sci. Technol. , vol. 5, no. 3, pp. 1360-1384, 2015.

[16] S. Rehman, R. Ullah, A. Butt, and N. D. Gohar, "Strategies of making TiO_2 and ZnO visible light active," J. Hazard. Mater. , vol. 170, no. 2-3, pp. 560-569, 2009.

[17] T. An et al., "Structural and photocatalytic hydrothermally treated mesoporous TiO_2," Appl. Catal. A Gen. , vol. 350, no. 2, pp. 237-243, 2008.

[18] P. Gharavi, S. M. Xie, L. Webster et al., "Interfacial origins of visible-light photocatalytic activity in ZnS–GaP multilayers," Acta Materialia , vol. 181, pp. 139-147, 2019.

[19] K. Edalati, R. Uehiro, S. Takechi et al., "Enhanced photocatalytic hydrogen production on GaN–ZnO oxynitride by introduction of strain-induced nitrogen vacancy complexes," Acta Materialia , vol. 185, pp. 149-156, 2020.

[20] S. Grimme, S. Ehrlich, and L. Goerigk, "Effect of the damping function in dispersion corrected density functional theory," J. Comput. Chem. , vol. 32, pp. 1456-1465, 2011.

[21] B. Bhuyan, B. Paul, and S. S. Dhar, "Cetyltrimethylammonium bromide promoted size tuning synthesis of rod-like $CuAl_2O_4$ nanoparticles and their catalytic studies in oxidative esterification of aldehydes," Nanosci. Nanotechnol. Lett. , vol. 8, pp. 344-353, 2016.

[22] A. H. Reshak, “Novel photocatalytic water splitting solar-to-hydrogen energy conversion: CdLa2S4 and CdLa2Se4 ternary semiconductor compounds,” Phys. Chem. Chem. Phys., vol. 20, no. 13, pp. 8848–8858, 2018.

[23] A. Mohamed, R. El-Sayed, T. A. Osman, M. S. Toprak, M. Muhammed, and A. Uheida, "Composite nanofibers for highly efficient photocatalytic degradation of organic dyes from contaminated water," Environ. Res. , vol. 145, pp. 18-25, 2016.

[24] D. A. Friesen, L. Morello, J. V. Headley, and C. H. Langford, "Factors influencing relative efficiency in photo-oxidations of organic molecules by $Cs_3PW_{12}O_{40}$ and TiO_2 colloidal photocatalysts," J. Photochem. Photobiol. A Chem. , vol. 133, no. 3, pp. 213-220, 2000.

[25] R. Vinu and G. Madras, "Photocatalytic degradation of water pollutants using nano-TiO_2," in Energy Efficiency and Renewable Energy Through Nanotechnology , Springer, 2011, pp. 625-677.

[26] S. Linic, P. Christopher, and D. B. Ingram, "Plasmonic-metal nanostructures for efficient conversion of solar to chemical energy," Nat. Mater. , vol. 10, no. 12, pp. 911-921, 2011.

[27] Y. Cai, X. Li, Y. Zhang, X. Wei, K. Wang, and J. Chen, "Highly efficient dehydrogenation of formic acid over a palladium-nanoparticle-based Mott-Schottky photocatalyst," Angew. Chem. Int. Ed., vol. 52, no. 3, pp. 12038-12041, 2013.

[28] B. Rusinque, "Hydrogen production by photocatalytic water splitting under near-UV and visible light using doped Pt and Pd TiO_2," 2018.

[29] J. Arana et al., "Photocatalytic degradation of formaldehyde containing wastewater from veterinarian laboratories," Chemosphere , vol. 55, no. 6, pp. 893-904, 2004.

[30] D. Jing et al., "Efficient solar hydrogen production by photocatalytic water splitting: from fundamental study to pilot demonstration," Int. J. Hydrogen Energy, vol. 35, no. 13, pp. 7087-7097, 2010.

[31] A .Kudo and Y. Miseki, "Heterogeneous photocatalyst materials for water splitting," Chem. Soc. Rev. , vol. 38, pp. 253-278, 2009.

[32] A. Fujishima, K. Hashimoto, and T. Watanabe, TiO_2 Photocatalysis: Fundamentals and Applications. BKC, Inc., 1999.

[33] A. B. Djurišić et al., "Photocatalytic mechanisms of zinc oxide: review," J. Photochem. Photobiol. C Photochem. Rev. , vol. 42, pp. 52-70, 2020.

[34] C. Pandis, K. Mogyorosi, Z. Pap, S. Djuric, and G. Zlatko, "Copper oxide modified titania: photocatalytic activity and stability," Catalysts, vol. 7, no. 3, p. 80, 2017.

[35] M. F. Hossain et al., "An overview on the role of nanostructures in the photocatalytic degradation of organic pollutants in wastewater," Environ. Technol. Innov. , vol. 22, p. 101525, 2021.

[36] M. Sathish, B. Viswanathan, R. P. Viswanath, and C. S. Gopinath, "Synthesis, characterization, electronic structure, and photocatalytic activity of nitrogen-doped TiO_2 nanocatalyst," Chem. Mater. , vol. 17, no. 25, pp. 6349-6353, 2005.

[37] A. H. Reshak, “Photocatalytic water splitting solar-to-hydrogen energy conversion: Perovskite-type hydride XBeH3 (X = Li or Na) as active photocatalysts,” J. Catal., vol. 351, pp. 119–129, 2017.

[38] M. J. Al-anber, A. M. Ali, N. S. Al-Mailky, and A. H. Al-Mowali, “Theoretical DFT Study the Opto-electronic Properties of Poly(3,4-Ethylenedioxythiophene),” Sci. World, vol. 11, no. 11, pp. 66–69, 2013, doi: 10.3126/sw.v11 i11.8555.

[39] Y. Shiraishi et al., "TiO_2-photocatalyzed H_2O_2 production from ethanol/O_2 system using metal nanoclusters as hydrogen-evolution co-catalysts," ACS Catal. , vol. 3, no. 11, pp. 2474-2481, 2013.

[40] A. H. Reshak and S. Auluck, “Photocatalytic water-splitting solar-to-hydrogen energy conversion: Novel LiMoO3(IO3) molybdenyl iodate based on WO3-type sheets,” J. Catal., vol. 351, pp. 1–9, 2017.

[41] W. Song et al., "Synthesis and photocatalytic activity of CdS/ZnS nanocomposites for organic dye degradation," J. Mater. Sci. , vol. 53, no. 15, pp. 10967-10975, 2018.

[42] A. Mills and S. LeHunte, "An overview of semiconductor photocatalysis," J. Photochem. Photobiol. A Chem., vol. 108, no. 1, pp. 1-35, 1997.

[43] B. Neppolian, H. Jung, S. Choi, and H. Kang, "TiO_2/zeolite composite for the photocatalytic degradation of organic pollutants in water," Water Res. , vol. 36, no. 7, pp. 1543-1548, 2002.

[44] P. Ivanov, D. Popov, A. Grozdanov, and T. Ivanova, "Synthesis and application of ZnO/Zeolite composite for photocatalytic degradation of organic pollutants in wastewater," Bulgarian Chemical Communications, vol. 52, pp. 497-503, 2020.

[45] G. Liu et al., "A review of semiconductor heterojunction photocatalysts: synthesis, characterization and applications," Chem. Eng. J., vol. 302, pp. 739-760, 2016.

[46] Z. Chen et al., "TiO_2 nanotube arrays and their use in dye-sensitized solar cells," Nat. Nanotechnol. , vol. 4, no. 1, pp. 836-840, 2009.

[47] H. Song, J. Wang, Z. Wu, J. Zheng, and X. Li, "ZnO: Carbon dot composite: enhanced photocatalytic activity and stability," Appl. Surf. Sci., vol. 396, pp. 1585-1592, 2017.

[48] Y. Liu, C. Chen, J. Cao, W. Shi, and S. Xu, "Recent advances in plasmonic metal/semiconductor composite nanomaterials: properties, synthesis and their applications," Mater. Today Energy, vol. 9, pp. 100-132, 2018.

[49] A. H. Reshak, "Sulfide oxide XZnSO (X = Ca or Sr) as novel active photocatalytic water splitting solar-to-hydrogen energy conversion," Appl. Catal. B Environ., vol. 225, no. December 2017, pp. 273–283, 2018.

[50] B. T. M. Willis, T. M. Hayes, and T. W. M. Coddington, "Structure and properties of copper aluminate," J. Phys. Chem. Solids, vol. 23, no. 10, pp. 1005-1010, 1962.

[51] W. Su, Y. Zhang, Y. Guo, X. Zhao, X. Zhang, and J. Zhao, "Low-temperature hydrothermal synthesis of $CuAl_2O_4$ nanocrystals: Structural, magnetic, and catalytic properties," J. Nanopart. Res. , vol. 13, no. 2, pp. 851-857, 2011.

[52] Y. Li, X. Fang, D. R. MacFarlane, and Z. Yan, "Efficient synthesis of $CuAl_2O_4$ nanoparticles using a facile microwave-assisted method," J. Am. Ceram. Soc., vol. 97, no. 2, pp. 412-415, 2014.

[53] A. S. Lanje, S. J. Sharma, R. S. Ningthoujam, J. S. V. Maitra, and R. B. Pode, "Synthesis and optical characterization of copper aluminate ($CuAl_2O_4$) spinel nanoparticles," Int. J. Nanotechnol. , vol. 8, no. 4, pp. 381-387, 2011.

[54] X. Pan, Y. Zhao, S. Liu, X. Feng, L. Tan, and X. Zhu, "Photocatalytic activity of $CuAl_2O_4$ nanoparticles under visible light irradiation," Ceram. Int., vol. 41, no. 1, pp. 991-996, 2015.

[55] F. Bahrani, R. Hameed, S. Resan, and M. Al-Anber, "Impact of Torsion Angles to Tune Efficient Dye-Sensitized Solar Cell/Donor-π-Acceptor Model Containing Triphenylamine: DFT/TD-DFT Study," Acta Phys. Pol. A, vol. 141, no. 6, pp. 561–568, 2022, doi: 10.12693/APhysPolA.141.561.

[56] X. Wang, H. Ouyang, X. Zhang, and S. Yang, "Visible light photocatalytic degradation of organic pollutants over $CuAl_2O_4$ nanostructures," Nanoscale Res. Lett. , vol. 12, no. 1, p. 45, 2017.

[57] K. J. Kim et al., "Mechanism of visible-light-driven photocatalytic degradation of organic pollutants over metal-doped TiO_2," J. Catal. , vol. 297, pp. 62-72, 2013.

[58] R. Chauhan, "$CuAl_2O_4$ nanoparticles for photocatalytic degradation of organic pollutants under visible light irradiation," J. Nanopart. Res., vol. 17, no. 1, p. 20, 2015.